GEOPHYSICAL RESEARCH LETTERS, VOL. 24, NO. 6, PAGES 639-642, MARCH 15, 1997

The seasonal and long term changes in mesospheric water vapor

S. Chandra[1], C. H. Jackman[1], E. L. Fleming[2] and J. M. Russell III[3]

Abstract: This study explores the feasibility of identifying long term changes in mesospheric water vapor as a result of increasing level of methane in the atmosphere and the solar cycle variation of Lyman α. The study is based on recent measurements of water vapor in the mesosphere and the solar Lyman α flux from the UARS (Upper Atmosphere Research Satellite) HALOE (Halogen Occultation Experiment) and the SOLSTICE (Solar Stellar Irradiance Comparison Experiment) instruments during the declining phase of the solar cycle 22. The solar activity during this period decreased from a near maximum to a near minimum level. The analysis of these data sets, in conjunction with the NASA/GSFC two dimensional chemistry and transport model suggests that on a seasonal time scale, the temporal changes in mesospheric water vapor are largely controlled by the vertical advection associated with the meridional circulation. On the time scale of a solar cycle, H_2O may vary by about 30-40 % near the mesopause height ($\sim$80 km) to about 1-2% in the lower mesosphere (60-65 km) caused by the solar cycle modulation of Lyman α. In comparison, the secular increase in H_2O related to methane increase in the atmosphere is about 0.4% /year at all heights in the mesosphere.

Introduction

A number of recent studies have suggested that the changes in mesospheric water vapor and temperature may be good indicators of anthropogenic increases in carbon dioxide (CO_2) and methane (CH_4) concentrations on climatic time scales [*Thomas*, 1996 and the references therein]. Water vapor has no known significant in-situ source in the mesosphere, but rather is transported upwards from the stratosphere via the meridional circulation and eddy transport. Water vapor in the stratosphere is produced by a combination of upward transport through the tropical tropopause and in-situ oxidation of methane. Since methane is biologically produced and affected by humankind behavior, the long term changes in mesospheric water can be affected by the anthropogenic increases in the level of methane at the ground. At mesospheric heights, water vapor is strongly photo-dissociated by solar Lyman α [e.g., *Brasseur and Solomon*, 1986]. Therefore, solar cycle UV changes will have a strong influence on the long term changes in mesospheric water vapor in addition to the secular increase of water vapor due to methane increases. The H_2O sensitivity to Lyman α (% change in H_2O for a 1% increase in Lyman α), estimated from numerical models, varies from -.05 at about 0.1 hPa ($\sim$64 km) to almost -1.0 at about .01 hPa ($\sim$80 km) [see for example, *Fleming et al.*, 1995]. The variation in solar Lyman α flux measured by the UARS SOLSTICE instrument for the declining phase of solar cycle 22 is estimated to be 45% from a near maximum to a near minimum level of solar activity [*Chandra et al.*, 1995]. Such a decrease should cause an increase of 2% in H_2O in the lower mesosphere and nearly 45% in the upper mesosphere near .01 hPa. This change should be detectable in the UARS measurements of H_2O from the HALOE experiment [*Russell et al.*, 1993], particularly near .01 hPa.

The purpose of this paper is to study the seasonal and long term changes in mesospheric water vapor associated with mesospheric dynamics, the solar cycle variation of Lyman α, and the increasing level of methane in the atmosphere. These variations in H_2O are computed with the Goddard 2-D model and are compared with changes in water vapor observed by HALOE from 1991 to 1995 [*Harries et al.*, 1996] when the solar activity, specifically the Lyman α flux, decreased from a near maximum to a near minimum level.

The model results are based on simulations run from 1955 to the present time [*Jackman et al.*, 1996] using time dependent source gas boundary conditions varied according to Table 3.2 of WMO [1989] for the years prior to 1970 and to Table 6-3 of WMO [1995] for years 1970 and after. This scenario assumes a methane increase at the ground of 0.7 to 1% per year with a larger percentage increase near the beginning of the simulation and a smaller increase near the end. The solar UV spectral model used in this study is based on the UARS SOLSTICE measurements in the 120-250 nm spectral range with 1 nm resolution. Using the F10.7 cm flux as a transfer standard, the solar UV model is extrapolated back in time to 1955 as discussed in *Jackman et al.* [1996]. The model results are compared with the HALOE H_2O data (version 18) to delineate the relative roles of mesospheric dynamics and photochemistry.

The GSFC 2-D Model

The GSFC 2-D model was originally described in *Douglass et al.* [1989], with inclusion of mesospheric processes described in *Jackman et al.* [1990] and *Fleming et al.* [1995]. More recently, improvements have been made to the model photolysis calculations and the transport algorithm which are now significantly different from previous versions [*Jackman et al.*, 1996]. The transport algorithm computes a meridional stream function to obtain the transformed Eulerian circulation ($\bar{v}^*$, $\bar{w}^*$). The coefficients of the elliptic stream function equation depend on the zonal mean temperature and zonal wind, which are based on the 17 year average (1979-1995) of data from the National Centers for Environmental Prediction (NCEP) for 1000-1 hPa, and the CIRA-86 empirical reference model for the mesosphere above 1 hPa. Zonal wind is derived from temperature using the thermal wind relation. Forcing of the stream function is proportional to the vertical gradient of the mechanical forcing from planetary and gravity waves and the latitudinal gradient of the total heating rate. Diabatic heating rates are computed following *Rosenfield et al.* [1994]. Forcing from planetary waves is proportional to the Eliassen-Palm (E-P) flux divergence [e.g., *Andrews et al.*, 1987], which we have computed offline from the 17-year NCEP 3-dimensional analyses for 1000-1 hPa and the CIRA-86 empirical reference model of planetary waves for the mesosphere. To obtain distributions of vertical eddy diffusion and mechanical forcing from gravity waves, we have incorporated into the model the parameterization developed by *Lindzen* [1981] and modified by *Holton and Zhu* [1984]. Here, we utilize the empirical zonal mean temperature and zonal wind fields (described above) in the parameterization to diagnose the latitudinal, seasonal, and vertical distributions of gravity wave drag and diffusion based on a given set of gravity wave parameters.

[1]Code 916; Goddard Space Flight Center, Greenbelt, Md. 20771
(e-mail: chandra@gsfc.nasa.gov)
[2] Applied Research Corporation, Corporate Drive, Landover, Md.,20785
[3]Physics Department, Hampton University, Hampton, Va., 23668

Paper number 97GL00546.
0094-8534/97/97GL-00546$05.00

In this paper it will be shown that in the context of mesospheric water vapor, this new circulation compares reasonably well with UARS HALOE observations and indicates that this circulation adequately represents zonal mean transport processes in the middle atmosphere. More detailed comparisons between long lived tracer distributions calculated with this new circulation and UARS observations will be discussed in a forth coming paper.

HALOE measurements of H_2O

The HALOE instrument on UARS measures the composition of the stratosphere and the mesosphere by measuring infrared radiation in the 2.5 to 10.0 μm region. The water vapor is measured by a broad band filter channel at 6.6 μm [*Harries et al.*, 1996]. HALOE is a solar occultation experiment and therefore the measurements are made only at sunrise and sunset. The latitudes of the sunrise and sunset change slowly with the drift of the UARS orbit. It takes a few weeks to build a global coverage. For this study, we have used the level 3A HALOE water vapor data (version 18) averaged in 10^0 degree latitude bins from 75°S to 75°N. Both sunrise and sunset measurements are used. In constructing the time series, the missing data have been linearly interpolated.

Model results and comparison with the HALOE measurements

Figure 1 shows the seasonal variation in H_2O mixing ratio from the model and the HALOE data from 1992 to 1995 at 45^{0}N and at 2 selected pressure levels, 0.1 hPa (~64 km) and 0.015 hPa (~77 km), respectively. Also shown in this figure are the monthly values of the vertical velocity($\overline{w}^*$) associated with the meridional circulation calculated in the model. Note that the $\overline{w}^*$ field is climatological and therefore does not vary from year to year.

Both the model and the observed H_2O in Figure 1 show a predominantly annual cycle of a comparable amplitude with an annual mean decreasing from about 5-5.5 ppmv at 64 km to about 2-2.8 ppmv at 77 km. In comparison, the annual amplitude increases from about 0.7 ppmv at 64 km to about 1.6 ppmv at 77 km. The seasonal characteristics of H_2O are similar to $\overline{w}^*$ with a phase lag of 1-2 months This phase lag is attributed to horizontal advection of H_2O . The variations in $\overline{w}^*$ reflect the rising motion during summer and sinking motion during winter characteristic of the seasonal variations of the mesospheric circulation [e.g., *Smith and Brasseur*, 1991; *Garcia et. al*, 1992; *Thomas*, 1996; *Summers et al., 1997*]. A time tendency analysis of water vapor computed in the model suggests that at mid-latitudes, the vertical advection term is significantly larger than the vertical diffusion term associated with gravity wave breaking as suggested by *Holton and Schoeberl* [1988]. This is illustrated in Figure 2 for the northern hemisphere summer (July). At mid and high latitudes the tendency term associated with vertical advection reaches a maximum of 0.7 ppmv/day at 70-85 km in northern hemisphere and a minimum of -0.35 ppmv/day in southern hemisphere. The corresponding values for vertical diffusion are in the range of 0.02 to 0.05 ppmv/day. The change in sign in Figure 2 (upper panel) is due to the change in sign of $\overline{w}^*$ from the summer to the winter and the decrease with altitude of mesospheric H_2O caused by the dissociation by Lyman α. Above 75 km, the sign of the vertical diffusion tendency term does not change and is positive in both the hemispheres.

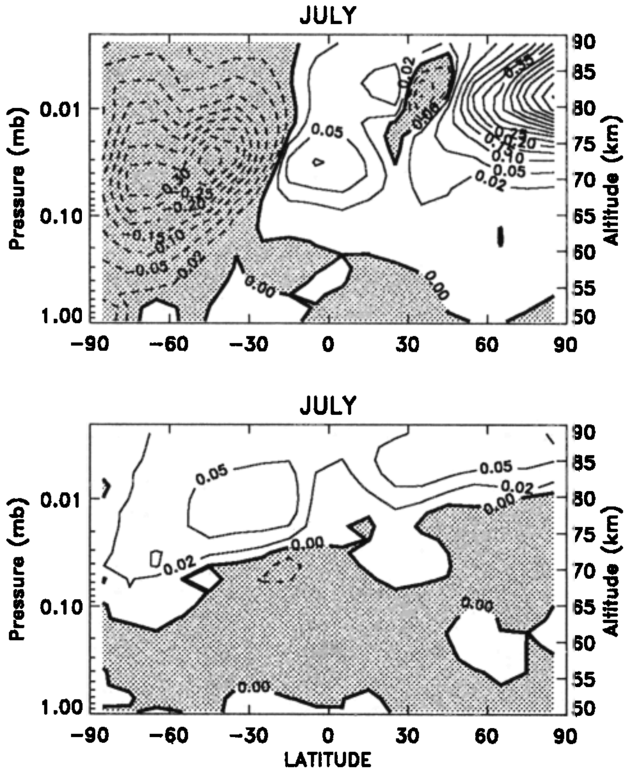

Figure 2. Time tendency of H_2O (ppmv/day) due to vertical advection (upper panel) and vertical diffusion (lower panel) for the month of July The contour interval is .05 ppmv for values < -.05 and > +.05 ppmv.

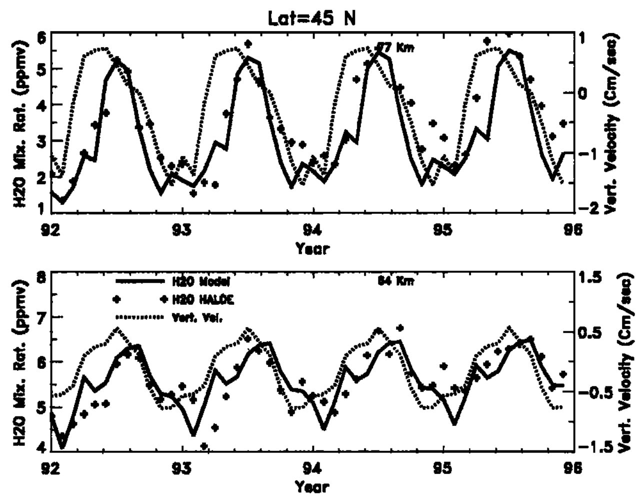

Figure 1. The seasonal variation in H_2O mixing ratio based on the model and the HALOE H_2O data from 1992 to 1995 at 45^{0}N and at 2 selected pressure levels, 0.1 hPa (~64 km) and 0.015 hPa (~77 km), respectively. Shown also are the monthly values of the vertical velocity($\overline{w}^*$) associated with the residual meridional circulation.

Figure 3 shows the HALOE and 2-D model H_2O at .01 hPa (~80 km) for three latitudes (45^{0}N, 5^{0}N, and 45^{0}S). The seasonal characteristics of the HALOE H_2O change from a predominantly annual cycle at the middle and high latitudes to a semi-annual cycle in the tropics. The model simulations are consistent with these observed seasonal characteristics, however, the absolute values of model H_2O do not always agree with the HALOE data and may differ by as much as 30% in the tropics.

A visual inspection of Figures 1 and 3 suggests an upward linear trend in H_2O superimposed on the annual and semi-annual cycles. For example, at 80 km and 45^{0}N (Figure 3, upper panel), the annually averaged H_2O mixing ratio inferred from the HALOE data increases from 2.41 to 3.22 ppmv from 1992 to 1995. The corresponding values inferred from the 2-D model are respectively 2.11 and 2.66 ppmv. Figure 4 shows the height profiles of the 4 year trend estimated from both the model and the HALOE data. These trends are calculated using a linear regression analysis. Before calculating trends, the time series are expressed in terms of % deviation with respect to the 4 year climatology and averaged

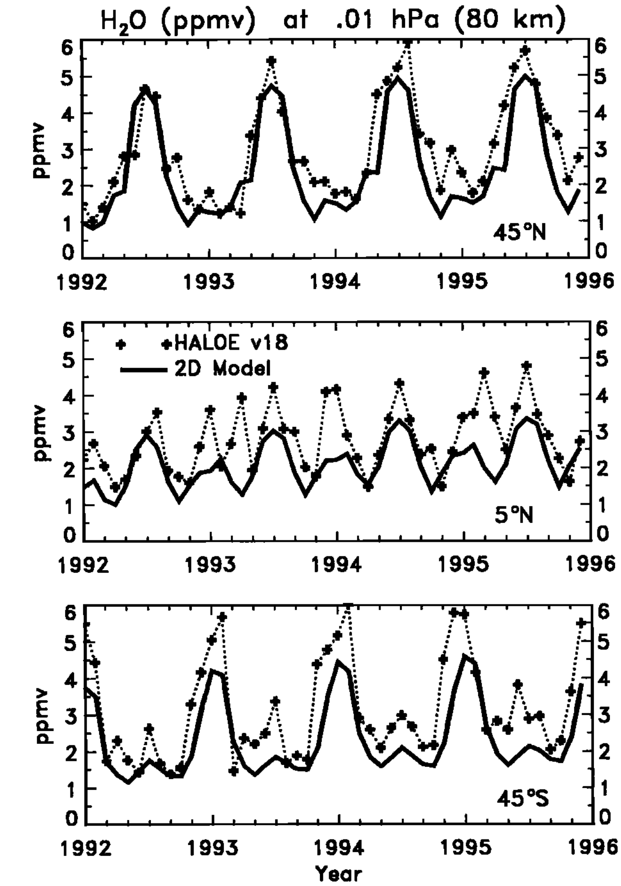

Figure 3. The seasonal variations of the HALOE and model H_2O at 0.01 hPa (~80 km) for three latitudes (45°N, 5°N, and 45°S).

from 60°S to 60°N (area weighted). As seen in Figure 4, the four year trends calculated from the 2-D model increase with height from 3% at .1 hPa to 34% at .01 hPa.

The contribution to the model H_2O trend throughout the mesosphere due to the increase in methane at the ground is determined as follows. At mesospheric heights in the model, virtually all of the methane has been destroyed through oxidation and photolysis and converted to water vapor, with a yield of two H_2O molecules created for one molecule of CH_4 destroyed. Given a methane input at the ground which increases with time from 1.57 ppmv in 1980 to 1.78 ppmv for 1995 conditions [WMO, 1995] the oxidation and photolysis of CH_4 yield about ~3-3.5 ppmv or roughly half of the total amount of water vapor in the lower mesosphere in the model. The other half is produced via upward transport through the tropical tropopause which varies seasonally but has no inter-annual time dependence. In terms of percentage change, an increase of about 0.8 % per year in methane input into the model causes an increase of about 0.4 % per year in mesospheric H_2O. This corresponds to an insrease of ~1.6% in H_2O over the four year period, 1992-1995. Therefore, roughly half of the model H_2O trend at 0.1 hPa of 3% in Figure 4 is due to the methane increase, with the other half due to the very small solar cycle Lyman α effect present at this level. As seen in Figure 4, the solar effect increases rapidly with height and is the predominant source of the trend in the middle and upper mesosphere, overwhelming the much smaller ~1.6% H_2O increase due to methane changes.

The four year trends inferred from the HALOE H_2O in Figure 4 are qualitatively similar to that of the model, increasing with height from about 10% at .1 hPa to 41% at .01 hPa, with a 2 σ error bar (95% confidence interval) which varies from about 2% to 8%. Given the uncertainties in the data and the relatively short four year data record, it is difficult to discern the expected small mesospheric H_2O trend due to methane increases in the HALOE observations. However, one would expect that the large H_2O trend in the upper mesosphere observed in the HALOE data is due primarily to the solar cycle effect, given the strong negative sensitivity of water vapor to solar Lyman α expected at these heights, and the fact that the Lyman α flux observed by UARS/SOLSTICE decreased significantly between 1992 and 1996 (see Figure 5).

Figure 4 also reveals that the modeled trends are systematically less than the observed trends by about 7% at all levels. Uncertainties in the data, and for example, in the H_2O photolysis rates used in the model, may cause some of this difference. However, a greater source of discrepancy may be due to inter-annual dynamical variability which may affect the HALOE trends because of the relatively short data record. Such variability is not contained in the model since it uses climatologically based transport fields.

A further insight into the Lyman α and methane related changes in H_2O on climatological time scales can be obtained from Figure 5. In this figure, we compare variations in the 2-D model H_2O from 1958 to 1995 and the HALOE H_2O from 1992 to 1995 with respect to Lyman α. The H_2O time series correspond to tropical latitudes (~5° N) at the 2 pressure levels .01 hPa (~ 80 km) and

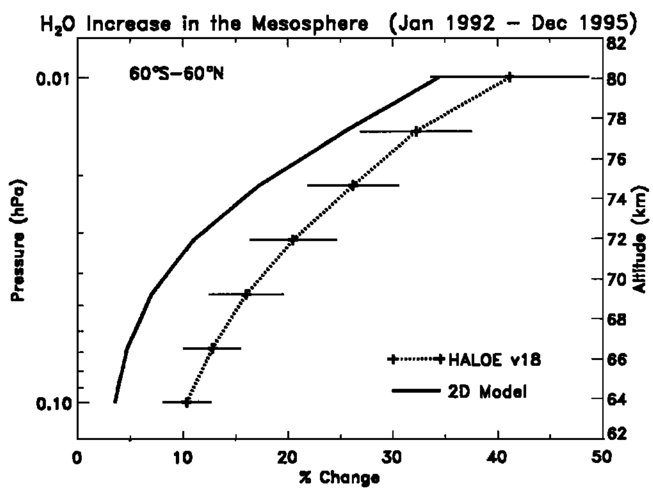

Figure 4. Height profiles of the 4 year trend estimated from both the model and the HALOE data averaged over 60°S to 60°N.

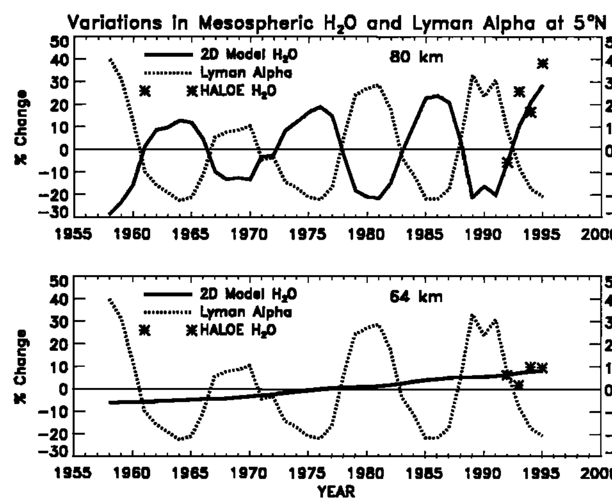

Figure 5. Relative variations of the modeled H_2O from 1958 to 1995 and the observed H_2O from the HALOE from 1992 to 1995 compared to Lyman α. The H_2O time series correspond to tropical latitudes (~5° N) at the 2 pressure levels, .01 hPa (~ 80 km) and 0.1 hPa (~64 km), respectively (see text for details).

0.1 hPa (~64 km), respectively. All the time series are based on annual averages and represent percentage change with respect to the 38 year average (1958-1995) for the model H_2O and Lyman α and the 1992 annual average for the HALOE H_2O. To facilitate the visual comparison, the HALOE data have been shifted by a constant at each altitude to coincide with 1992 model values. For the 2 pressure levels shown in Figure 5, these constants are respectively-5.5% at 0.01 hPa (upper panel) and 6.3 % at 0.1 hPa (lower panel).

The upper panel in Figure 5 shows a strong solar cycle modulation of H_2O at .01 hPa (~80 km) which is out of phase with Lyman α over the four solar cycles used in this simulation. As discussed above, this modulation becomes weaker with decreasing height and is almost undetectable at 0.1 hPa (lower panel). At 0.1 hPa, where the solar effects are very small, the H_2O time series shows mostly a secular increase of 0.4-0.5 % per year. A regression analysis of the model H_2O time series suggests a linear trend of about 0.4 % per year at all levels in the mesosphere which is consistent with the methane increase of 0.7 to 1 % per year input into the model, as discussed earlier in this paper. Over the four year period of the UARS measurements, the HALOE H_2O trends are qualitatively consistent with the model trends as in Figure 4. However, because of the strong solar influence, they should not be characterized as trends but simply changes induced by the photo-dissociation of Lyman α.

Figure 5 illustrates the difficulty of separating the methane related changes from those produced by solar Lyman α in the upper mesosphere even when the measurements are made over an extended period. In this region, the solar cycle related changes in water far exceed the methane related changes. Another difficulty is that the solar cycle modulation of H_2O is not the same from one solar cycle to another because of the differences in the level of solar activity. This has the potential of introducing a trend in H_2O unrelated to the methane increase. The best chance of detecting the methane related change in H_2O, therefore, appears to be in the lower mesosphere (60-65 km) where the solar effects are relatively small.

Conclusion

In this paper we have studied the seasonal and long term changes in mesospheric H_2O induced by atmospheric dynamics, the solar cycle variation of Lyman α, and the increasing level of methane in the atmosphere. Our study shows that the seasonal characteristics of the water vapor in the mesosphere, inferred from both the HALOE measurements and the GSFC 2-D chemistry and transport model, are very similar. They both change from a predominantly annual cycle at middle and high latitudes to a semi-annual cycle in the tropics. The seasonal changes in H_2O are consistent with seasonal changes in vertical advection by the mean meridional circulation. Our study also suggests that the role of vertical diffusion induced by breaking gravity waves is relatively minor compared to the advective contribution. Similar conclusions have been arrived at in a number of recent studies of the seasonal variations of mesospheric water vapor based on ground based measurements [e.g. Nedoluha et al., 1996 and the references therein].

On longer time scales, the solar cycle variation of Lyman α has a strong modulating influence on the secular trend in H_2O caused by the increasing level of CH_4 on the surface of the earth. On the time scales of a solar cycle, the solar related changes in H_2O may vary by 30-40 % near the mesopause compared to the methane related changes of about 4-5 %. The latter effect, therefore, is mostly masked by the solar cycle effect and may not be detectable even when the measurements extend over more than a solar cycle. This task is further complicated due to the lack of our understanding of dynamical processes both in the troposphere and middle atmosphere which may also contribute to long term changes in mesospheric H_2O. In spite of these difficulties, the long term monitoring of H_2O may offer an opportunity for detecting climatic signals in the lower mesosphere where the CH_4 and the solar cycle related changes are comparable.

Acknowledgment. We would like to acknowledge helpful discussions with Jerry R. Ziemke.

References

Andrews, D.G., J.R. Holton, and C.B. Leovy, Middle Atmosphere Dynamics, 498 pp., *Academic Press*, San Diego, Calif., 1987.

Brasseur, G. And S. Solomon, Aeronomy of the middle atmosphere, Second Edition, *Reidel*, 1986.

Chandra, S. J. L. Lean, O. R. White, D. K. Prinz, G. J. Rottman, and G. E. Brueckner, Solar UV irradiance variability during declining phase of the solar cycle 22, *Geophys. Res. Lett.*, *22*, 2481-2484, 1995.

Douglass, A.R., C.H. Jackman, R.S. Stolarski, Comparison of model results transporting the odd nitrogen family with results transporting separate odd nitrogen species, *J. Geophys. Res.*, *94*, 9862-9872, 1989.

Fleming, E.L., S. Chandra, C.H. Jackman, D.B. Considine, and A.R. Douglass, The middle atmospheric response to short and long term solar UV variations: Analysis of observations and 2-D model results, *J. Atmos. Terr. Phys.*, *57*, 333-365, 1995.

Garcia, R. J., F. Strodal, S. Solomon, and J. T. Kiehl, A numerical model of the middle atmosphere, 1. Dynamics and transport of the trace gases, *J. Geophys. Res.*,*97*, 12,967-12,991, 1992.

Harries et al., Validation of water vapor from the HALOGEN Occultation Experiment (HALOE), *J. Geophys. Res.*,*101*, 10205-10216, 1996.

Holton, J. R., and X. Zhu, A further study of gravity wave induced drag and diffusion in the mesosphere, *J. Atmos. Sci.*, *41*, 2653-2662, 1984

Holton J. R., and M. R. Schoeberl, The role of gravity wave generated advection and diffusion in transport of tracers in the mesosphere, *J. Geophys. Res.*,*93*, 11075-11082, 1988.

Jackman, C. H., A. R. Douglass, R. B. Rood, R. D. McPeters, and P. E. Meade. Effect of solar proton events in the middle atmosphere during the past two solar cycles as computed using a two dimensional model, *J. Geophys. Res.*, *95*, 7417-7428, 1990.

Jackman, C. H., E. L. Fleming, S. Chandra, D. B. Considine, and J. E. Rosenfield, Past, present, and future modeled ozone trends with comparisons to observed trends, *J. Geophys. Res.*, *101*, 28,753-28,767, 1996 .

Lindzen, R. S. ,Turbulence and stress owing to gravity wave and tidal breakdown, *J. Geophys. Res.*, *86*, 9707-9714, 1981.

Nedoluha et al., Measurements of water vapor in the middle atmosphere and the implications of mesospheric transport, *J. Geophys. Res.*, *101*, 21,183-21,193, 1996.

Rosenfield, J. E., P. A. Newman, and H. R. Schoeberl, Computations of diabatic descent in the stratospheric polar vortex, *J. Geophys. Res.*, *99*, 16677-16689, 1994.

Russell III et al., The Halogen Occultation Experiment, *J. Geophys. Res.*,*98*, 10,777-10,797, 1993.

Summers et al., Seasonal variations of the middle atmosphere CH_4 and H_2O with a new chemical and dynamical model, *J. Geophys. Res.*,*102*, 1997 (in press).

Smith, A. K., and G. P. Brasseur, Numerical simulation of the seasonal variation of mesospheric water vapor, *J. Geophys. Res.*,96, 7553-7563, 1991.

Thomas, G. E., Global change in the mesosphere-lower thermosphere region: has it already arrived, J. Atmos. Terr. Phys., 58, 1629-1656, 1996.

World Meteorological Organization (WMO), Scientific assessment of stratospheric ozone: 1989, Rep. 20, *Global Res. And Monit. Proj.*, Geneva, 1989.

World Meteorological Organization (WMO), Scientific assessment of stratospheric ozone: 1994, Rep. 37, *Global Res. And Monit. Proj.*, Geneva, 1995.

(Received December 30, 1996; revised February 20, 1997;
accepted February 24, 1997.)